

1 **Human coronavirus NL63 utilize heparan sulfate proteoglycans for attachment to target**
2 **cells**

3 Aleksandra Milewska^a, Mirosław Zarebski^b, Paulina Nowak^a, Karol Stozek^a, Jan Potempa^{a,c},
4 Krzysztof Pyrc^{a,d,#}

5 ^a Microbiology Department, Faculty of Biochemistry Biophysics and Biotechnology,
6 Jagiellonian University, Gronostajowa 7, 30-387 Krakow, Poland.

7 ^b Division of Cell Biophysics, Faculty of Biochemistry, Biophysics and Biotechnology,
8 Jagiellonian University, Krakow, Poland.

9 ^c Oral Health and Systemic Disease Research Group, School of Dentistry, University of
10 Louisville, Louisville, KY, USA

11 ^d Malopolska Centre of Biotechnology, Jagiellonian University, Gronostajowa 7, 30–387
12 Krakow, Poland

13

14

15

16

17

18

19

20

21

22 Word count:

23 1. Abstract: 152 + 114

24 2. Main text: 4 461

25

26

27

28 # Corresponding author: Krzysztof Pyrc, Microbiology Department, Faculty of Biochemistry
29 Biophysics and Biotechnology, Jagiellonian University, Gronostajowa 7, 30-387 Krakow,
30 Poland; Phone number: +48 12 664 61 21; Fax: +48 12 664 69 02.

31 E-mail: k.a.pyrc@uj.edu.pl

32 **ABSTRACT**

33 Human coronavirus NL63 (HCoV-NL63) is an alphacoronavirus that was first
34 identified in 2004 in the nasopharyngeal aspirate from a 7-month-old patient with a
35 respiratory tract infection. Previous studies showed that HCoV-NL63 and the genetically
36 distant SARS-CoV employ the same receptor for host cell entry, angiotensin converting
37 enzyme 2 (ACE2), but it is largely unclear whether ACE2 interactions are sufficient to allow
38 HCoV-NL63 binding to cells. The present study showed that directed expression of
39 angiotensin-converting enzyme 2 (ACE2) on cells previously resistant to HCoV-NL63
40 renders them susceptible, showing that ACE2 protein acts as a functional receptor and its
41 expression is required for infection. However, comparative analysis showed that directed
42 expression or selective scission of the ACE2 protein had no measurable effect on virus
43 adhesion. In contrast, binding of HCoV-NL63 to heparan sulfates was required for viral
44 attachment and infection of target cells, showing that these molecules serve as attachment
45 receptors for HCoV-NL63.

46 **IMPORTANCE**

47 ACE2 protein has been proposed as a receptor for HCoV-NL63 already in 2005, but the
48 in-depth analysis of early events during virus infection was not performed thus far. Here, we
49 show that the ACE2 protein is required for viral entry, but it is not the primary binding site on
50 the cell surface. Conducted research showed that heparan sulfate proteoglycans function as
51 adhesion molecules, increasing the virus density on cell surface and possibly facilitating
52 interaction between HCoV-NL63 and its receptor. Obtained results show that the initial
53 events during HCoV-NL63 infection are more complex than anticipated and newly described
54 interaction may be essential for understanding the infection process and, possibly, also assist
55 in the drug design.

56

57

58

59

60

61

62

63

64

65

66

67 **Keywords:** coronavirus, coronaviruses, virus, HCoV-NL63, attachment, receptor, ACE2,
68 angiotensin converting enzyme 2, heparan sulfate proteoglycans, heparan sulfate.

69

70 **INTRODUCTION**

71 Coronaviruses (CoVs) are enveloped positive-stranded RNA viruses with large
72 genomes ranging in size from 27 to 32 kb. Six human coronaviruses have been identified to
73 date, and four of them (HCoV-229E, HCoV-OC43, HCoV-NL63, and HCoV-HKU1) are
74 thought to be responsible for ~30% of common cold cases (1). By contrast, infection with
75 severe acute respiratory syndrome coronavirus (SARS-CoV) results in a serious respiratory
76 tract infection, which in 2002-2003 season affected approximately 8 000 patients with a
77 mortality rate of ~10% (2, 3). Similarly, the recently isolated Middle East respiratory
78 syndrome coronavirus (MERS-CoV) causes life-threatening pneumonia and renal failure,
79 with almost 300 fatal cases reported to date (4).

80 Human coronavirus NL63 was first identified in 2004 in the nasopharyngeal aspirate
81 from a 7-month-old patient with a respiratory tract infection. The virus is distributed
82 worldwide and causes respiratory infections of varying severity, with the most severe
83 symptoms seen in children and immunocompromised patients (5-9).

84 Like other human coronaviruses, the HCoV-NL63 genome encodes a glycoprotein,
85 called the spike (S) protein, which protrudes from the virion surface, thereby conferring the
86 corona-like form (6, 10, 11). The S protein is the main mediator of viral entry and determines
87 the host tropism of the coronavirus (12, 13). A study undertaken in 2005 used retroviral
88 reporter pseudoviruses carrying the HCoV-NL63 spike protein to show that HCoV-NL63
89 engages the SARS-CoV receptor, angiotensin-converting enzyme 2 (ACE2), for infectious
90 entry (14-16). ACE2 is a type I integral membrane protein abundantly expressed in tissues
91 lining the respiratory tract. This carboxypeptidase cleaves angiotensin II and functions within
92 the renin angiotensin system (RAS) important for maintaining lung homeostasis and blood
93 pressure (17-19). Down-regulation of ACE2 protein levels may lead to the development of

94 acute respiratory distress syndrome. Thus, down-regulation of ACE2 expression in the lungs
95 upon SARS-CoV infection is associated with viral pathogenesis (20-23).

96 HCoV-NL63 can be cultured in monkey epithelial cells lines that endogenously express
97 ACE2 (e.g., LLC-Mk2, Vero E6, or Vero B4 cells), as well as in the human hepatoma cell
98 line, Huh-7; this host preference is shared with SARS-CoV (24-26). Hofmann *et al.* (14)
99 conducted a thorough analysis of the cellular tropism of these two human coronaviruses and
100 found out that pseudovirions bearing the spike proteins of HCoV-NL63 (NL63-S) and
101 SARS-CoV (SARS-S) showed a similar ability to infect target cells. However, some studies
102 show that SARS-CoV S protein has a higher affinity for ACE2 than the HCoV-NL63 S
103 protein (20, 27).

104 Even though the cellular receptor for the HCoV-NL63 was described, until present it was
105 unknown whether it may serve as an adhesion factor and is sufficient to facilitate viral entry.
106 Here, we show that directed expression of the ACE2 protein renders the cells permissive to
107 HCoV-NL63 infection. Interestingly, the presence of the receptor protein seems not to
108 correlate with the adhesion of virions to cell surface, hence suggesting presence of yet another
109 factor important during early stages of infection. Subsequent analysis showed that heparan
110 sulfate (HS) proteoglycans function as adhesion receptors for HCoV-NL63, complementing
111 the action of the ACE2 protein. Assessment of viral replication dynamics clearly shows that
112 the adhesion of HCoV-NL63 to heparin sulfate proteoglycans enhances viral infection.

113 **MATERIALS AND METHODS**

114 *Cell culture*

115 LLC-Mk2 cells (ATCC: CCL-7; *Macaca mulatta* kidney epithelial) were maintained in
116 minimal essential medium (MEM; two parts Hanks' MEM and one part Earle's MEM; Life
117 Technologies, Poland) supplemented with 3% heat-inactivated fetal bovine serum (Life
118 Technologies, Poland), penicillin (100 U ml⁻¹), streptomycin (100 µg ml⁻¹) and ciprofloxacin
119 (5 µg ml⁻¹). Human 293T (ATCC: CRL-3216; kidney epithelial), A549 (ATCC: CCL-185;
120 lung carcinoma) were maintained in Dulbecco's MEM (Life Technologies, Poland)
121 supplemented with 10% heat-inactivated fetal bovine serum (Life Technologies, Poland),
122 penicillin (100 U ml⁻¹), streptomycin (100 µg ml⁻¹), and ciprofloxacin (5 µg ml⁻¹). Cells were
123 cultured at 37°C under 5% CO₂.

124

125 *Isolation of nucleic acids and reverse transcription*

126 HCoV-NL63 nucleic acids were isolated from cell culture supernatants using the Total
127 RNA Mini-Preps Super Kit (Bio Basic, Canada), according to the manufacturer's instructions.
128 Reverse transcription was carried out with a High Capacity cDNA Reverse Transcription Kit
129 (Life Technologies, Poland), according to the manufacturer's instructions.

130

131 *Cell lines expressing ACE2*

132 293T cells (ATCC CRL-3216) were transfected with the pLKO.1-TRC-ACE2 plasmid
133 using polyethylenimine (PEI; Sigma-Aldrich, Poland). The plasmid was based on the
134 Addgene plasmid 10878 (28). At 24 h post-transfection, the cells were washed with sterile
135 1 × PBS and cultured at 37°C for 48 h in media supplemented with puromycin (2 µg ml⁻¹) at
136 37°C with 5% CO₂. Following selection, cells were passaged and the surviving clones were
137 collected and analyzed as described below. ACE2-expressing (ACE2⁺) cells were maintained

138 in Dulbecco's MEM supplemented with 10% heat-inactivated fetal bovine serum, penicillin
139 (100 U ml^{-1}), streptomycin ($100 \mu\text{g ml}^{-1}$), ciprofloxacin ($5 \mu\text{g ml}^{-1}$) and puromycin ($1 \mu\text{g ml}^{-1}$).

140 ACE2-expressing A549 cells (A549_ACE2⁺) were generated using retroviral vectors
141 that were based on the Moloney Murine Leukemia Virus system. Briefly, Phoenix-Ampho
142 cells (ATCC CRL-3213) were transfected with a pLNCX2 vector (Clontech, USA) encoding
143 the ACE2 protein using PEI. At 24 h post-transfection the medium was refreshed and the cells
144 were cultured for a further 24 h at 32°C. Subsequently, the vector-containing supernatants
145 were harvested, aliquoted, and stored at -80°C .

146 A549_WT cells were cultured in six-well plates (TPP, Switzerland) and infected with
147 1 ml of generated retroviruses in the presence of polybrene ($5 \mu\text{g ml}^{-1}$, Sigma-Aldrich). After
148 24 h incubation at 37°C, the cells were cultured medium supplemented with G418 (BioShop,
149 Canada; 5 mg ml^{-1}) and passaged for 3 weeks at 37°C. Surviving clones were recovered and
150 analyzed as described below. A549_ACE2⁺ cells were maintained in Dulbecco's MEM
151 supplemented with 10% heat-inactivated fetal bovine serum, penicillin (100 U ml^{-1}),
152 streptomycin ($100 \mu\text{g ml}^{-1}$), ciprofloxacin ($5 \mu\text{g ml}^{-1}$) and G418 (5 mg ml^{-1}).

153

154 *Virus preparation, titration, and cell infection*

155 The HCoV-NL63 stock (isolate Amsterdam 1) was generated by infecting monolayers
156 of LLC-Mk2 cells. Cells were then lysed by two freeze-thaw cycles at 6 days
157 post-infection (p.i.). The virus-containing liquid was aliquoted and stored at -80°C . A control
158 LLC-Mk2 cell lysate from mock-infected cells was prepared in the same manner. The virus
159 yield was assessed by titration on fully confluent LLC-Mk2 cells in 96-well plates, according
160 to the method of Reed and Muench (29). Plates were incubated at 32°C for 6 days and the
161 cytopathic effect (CPE) was scored by observation under an inverted microscope.

162 In subsequent experiments, fully confluent cells (293T_WT/ACE2⁺ and
163 A549_WT/ACE2⁺) in six-well plates (TPP) were exposed to HCoV-NL63 at a TCID₅₀ ml⁻¹ of
164 5 000. HCoV-NL63-permissive LLC-Mk2 cells were infected with the virus at a TCID₅₀ ml⁻¹
165 of 400. Following a 2 h incubation at 32°C, unbound viruses were removed by washing with
166 sterile 1 × PBS and fresh medium was added to each well. Samples of cell culture supernatant
167 were collected every 24 h for 6 days and analyzed by real-time PCR.

168

169 *Quantitative PCR*

170 The virus yield was determined using real-time PCR (7500 Fast Real-Time PCR
171 machine; Life Technologies, Poland). Viral cDNA (2.5 µl per sample) was amplified in a
172 10 µl reaction mixture containing 1 × TaqMan Universal PCR Master Mix
173 (Life Technologies, Poland), specific probes labeled with 6-carboxyfluorescein (FAM) and
174 6-carboxytertamethylrhodamine (TAMRA) (100 nM), and primers (450 nM each). The
175 following primers were used for HCoV-NL63 amplification: sense, 5' – AAA CCT CGT
176 TGG AAG CGT GT - 3'; antisense, 5' – CTG TGG AAA ACC TTT GGC ATC - 3', probe,
177 5' – FAM -ATG TTA TTC AGT GCT TTG GTC CTC GTG AT – TAMRA - 3'. Rox was
178 used as the reference dye. The reaction conditions were as follows: 2 min at 50°C and 10 min
179 at 92°C, followed by 40 cycles of 15 sec at 92°C and 1 min at 60°C.

180

181 *Gradient purification of HCoV-NL63*

182 The virus stock was concentrated 25-fold using centrifugal protein concentrators
183 (Amicon Ultra, 10 kDa cut-off; Merck, Poland) and subsequently layered onto a 15%
184 iodixanol solution in 1 × PBS (OptiPrep medium; Sigma-Aldrich, Poland). Following
185 centrifugation at 175 000 × g for 3 h at 4°C (cushion), virus-containing fractions were layered
186 onto a 10-20% iodixanol gradient (in 1 × PBS) and centrifuged at 175 000 × g for 18 h at 4°C.

187 Fractions collected from the gradient were analyzed by Western blotting, followed by
188 detection of the HCoV-NL63 nucleocapsid protein. The resulting virus-containing fractions
189 were aliquoted and stored at -80°C . The control cell lysate (mock) was prepared in the same
190 manner as the virus stock.

191

192 ***Detection of sub-genomic mRNAs***

193 Total nucleic acids were isolated from virus- and mock-infected cells 5 days p.i. using
194 the Total RNA Mini-Preps Super Kit (Bio Basic, Canada), according to the manufacturer's
195 instructions. Reverse transcription was performed using a High Capacity cDNA Reverse
196 Transcription Kit (Life Technologies, Poland), according to the manufacturer's instructions.
197 Viral cDNA (3 μl) was amplified in a 20 μl reaction mixture containing 1 \times Dream Taq Green
198 PCR Master Mix and primers (each primer was used at 500 nM). The following primers were
199 used to amplify HCoV-NL63 sub-genomic (sg) mRNA: common sense primer (leader
200 sequence), 5' – TAA AGA ATT TTT CTA TCT ATA GAT AG – 3'; 1a/b polyprotein
201 antisense, 5' – CAT CAA AGT CCT GAA GAA CAT AAT TG – 3'; spike antisense, 5' –
202 ACT ACG GTG ATT ACC AAC ATC AAT ATA – 3'; spike (nested PCR) antisense, 5' –
203 AGA GAT TAG CAT TAC TAT TAC ATG TG – 3'; ORF3 antisense, 5' – GCA CAT AGA
204 CAA ATA GTG TCA ATA GT – 3'; envelope antisense, 5' – GCT ATT TGC ATA TAA
205 TCT TGG TAA GC – 3'; membrane antisense, 5' – GAC CCA GTC CAC ATT AAA ATT
206 GAC A – 3'; nucleocapsid antisense, 5' – CTT ATG AGG TCC AGT ACC TAG GTA AT –
207 3'. The conditions were as follows: 3 min at 95°C , 40 cycles (30 cycles for nested PCR) of
208 30 sec at 95°C , 30 sec at 47°C and 25 sec at 72°C , and then 5 min at 72°C and 10 min at 4°C .
209 The PCR products were run on 1% agarose gels (1 \times TAE buffer) and analyzed using
210 Molecular Imaging Software (Kodak).

211

212 **Western blot analysis**

213 Cells used for Western blot analysis were harvested at 5 days p.i. by scraping in ice-cold
214 $1 \times$ PBS. The cells were then centrifuged and resuspended in RIPA buffer (50 mM Tris,
215 150 mM NaCl, 1% Nonidet P-40, 0.5% sodium deoxycholate, 0.1% SDS, pH 7.5) followed
216 by lysis in RIPA buffer for 30 min on ice. Subsequently, samples were centrifuged (10 min at
217 $12\,000 \times g$) and the pelleted cell debris was discarded. Total protein concentration of each
218 sample was quantified using the BCA method and the resulting supernatants were mixed with
219 sample buffer (0.5 M Tris pH 6.8, 10% SDS, 50 mg/ml DTT), boiled for 5 min, cooled on ice,
220 and separated on 10% polyacrylamide gels alongside dual color Page Ruler Pre-stained
221 Protein size markers (Thermo Scientific, Poland). The separated proteins were then
222 transferred onto a Westran S PVDF membrane (Whatman) by semi-dry blotting (Bio-Rad) for
223 1.5 h, 100 Volts in transfer buffer: 25 mM Tris, 192 mM glycine, 20% methanol at 4°C. The
224 membranes were then blocked by overnight incubation (at 4°C) in TBS-Tween (0.1%) buffer
225 supplemented with 5% skimmed milk (BioShop, Canada). A goat anti-human ACE2
226 ectodomain antibody ($2 \mu\text{g ml}^{-1}$; R&D Systems, USA) and horseradish peroxidase-labeled
227 rabbit anti-goat IgG (26 ng ml^{-1} ; Dako, Denmark) were used to detect the ACE2 protein in
228 human cell lysates and cell supernatants. A mouse anti-HCoV-NL63-N protein antibody
229 (500 ng ml^{-1} ; Ingenansa, Spain) and horseradish peroxidase-labeled rabbit anti-mouse IgG
230 (65 ng ml^{-1} ; Dako, Denmark) were used to detect the HCoV-NL63 nucleocapsid protein. A
231 mouse anti- β -actin antibody (50 ng ml^{-1} ; BD Biosciences, USA) and horseradish peroxidase-
232 labeled rabbit anti-mouse IgG (65 ng ml^{-1} ; Dako, Denmark) were used for detection of β -
233 actin. All antibodies were diluted in 1% skimmed milk/TBS-Tween (0.1%). The signal was
234 developed using the Immobilon Western Chemiluminescent HRP Substrate (Millipore) and
235 visualized by exposing the membrane to an X-ray film (Kodak).

236

237 ***Flow cytometry***

238 A549-WT/ACE2⁺ and LLC-Mk2 cells were seeded in six-well plates (TPP,
239 Switzerland), cultured for 2 days at 37°C, and stimulated with PMA (phorbol 12-myristate
240 13-acetate; 1 µM; Sigma-Aldrich, Poland) for 1 h at 37°C. To examine HCoV-NL63
241 adhesion, cells were washed with 1 × PBS and incubated with iodixanol-concentrated
242 HCoV-NL63 or mock control for 2 h at 4°C. The cells were then washed with 1 × PBS, fixed
243 with 3% PFA, permeabilized with 0.1% Triton X-100 in 1 × PBS, and incubated for 1 h with
244 3% BSA/0.1% Tween 20 in 1 × PBS. To examine the HCoV-NL63 adhesion, cells were
245 mechanically detached from the plate surface and incubated for 2 h at room temperature with
246 a mouse anti-HCoV-NL63-N antibody (1 µg ml⁻¹; Ingenansa, Spain), followed by a 1 h
247 incubation with an Alexa Fluor 488-labeled goat anti-mouse antibody (2.5 µg ml⁻¹; Molecular
248 Probes). For ACE2 staining, cells were washed with 1 × PBS, scraped from the plates, and
249 incubated for 2 h at 4°C with goat anti-ACE2 ectodomain IgG (4 µg ml⁻¹; R&D Systems,
250 USA), followed by a 1 h incubation with an FITC-labeled rabbit anti-goat IgG antibody
251 (13 µg ml⁻¹; Dako, Denmark). Cells were then washed, resuspended in 1 × PBS and analyzed
252 by flow cytometry (FACSCalibur, Becton Dickinson). Data were analyzed using Cell Quest
253 software (Becton Dickinson).

254

255 ***Confocal microscopy***

256 LLC-Mk2 cells were seeded on coverslips in six-wells plates (TPP), cultured for 2 days
257 at 37°C and then stimulated with PMA (1 µM; Sigma-Aldrich, Poland) for 1 h at 37°C.
258 Subsequently, the cells were washed with 1 × PBS and incubated with iodixanol-concentrated
259 HCoV-NL63 or mock control for 2 h at 4°C. Cells were then washed with 1 × PBS, fixed
260 with 3% PFA, permeabilized with 0.1% Triton X-100 in 1 × PBS and incubated for 1 h with
261 5% BSA / 0.5% Tween 20 in 1 × PBS. To visualize HCoV-NL63 adhesion, cells were

262 incubated for 2 h at room temperature with mouse anti-NL63-N IgG (0.25 $\mu\text{g ml}^{-1}$; Ingenansa,
263 Spain), followed by a 1 h incubation with Alexa Fluor 488-labeled goat anti-mouse IgG
264 (2.5 $\mu\text{g ml}^{-1}$, Life Technologies, Poland). Nuclear DNA staining was performed with DAPI
265 (0.1 $\mu\text{g ml}^{-1}$, Sigma-Aldrich, Poland). Immunostained cultures were mounted on glass slides
266 in Vectashield medium (Vector Laboratories, UK). Fluorescent images were acquired under a
267 Leica TCS SP5 II confocal microscope (Leica Microsystems GmbH, Mannheim, Germany).
268 Images were acquired using Leica Application Suite Advanced Fluorescence LAS AF v. 2.2.1
269 (Leica Microsystems CMS GmbH), deconvolved with Huygens Essential package ver. 4.4
270 (Scientific Volume Imaging B.V.; The Netherlands) and processed using ImageJ 1.47v
271 (National Institutes of Health, Bethesda, Maryland, USA). Viruses attached to the cell were
272 quantified using 3D Object Counter ImageJ plugin (30) with the histogram threshold set
273 to 80. Analysis was performed on z-stacks (step size: 0.13 μm) of at least 10 cells per sample.

274

275 *Assessing the effects of neuraminidase on virus adherence*

276 LLC-Mk2 cells were seeded in six-well plates (TPP, Switzerland), cultured for 2 days at
277 37°C, and incubated with type V neuraminidase (from *Clostridium perfringens*;
278 100-200 mU/ml; Sigma-Aldrich, Poland) for 1 h at 37°C. The adherence of
279 iodixanol-concentrated HCoV-NL63 was examined as described above.

280

281 *Assessing the effects of sugars and heparan sulfate on virus replication and adherence*

282 LLC-Mk2 cells were seeded in six-well plates (TPP, Switzerland), cultured for 2 days
283 at 37°C, and incubated with sugar monomers (50 mM; Sigma-Aldrich, Poland) or heparan
284 sulfate - HS (Sigma-Aldrich, Poland) for 1 h at 37°C. Simultaneously, iodixanol-concentrated
285 HCoV-NL63 was incubated with tested compounds for 1 h at 4°C, and virus adherence was
286 examined as described above. To assess HCoV-NL63 replication, cells were washed with

287 1 × PBS and infected with virus pre-incubated with HS at a TCID₅₀ ml⁻¹ of 100. Following a
288 2 h incubation at 32 °C, unbound virus was removed by washing with 1 × PBS and fresh
289 medium containing HS was added to each well. Samples of cell culture supernatant were
290 collected 6 days post-infection and analyzed in a real-time PCR assay.

291

292 **RESULTS**

293 *Development of cell lines expressing the ACE2 protein*

294 Human cell lines stably expressing the ACE2 receptor (A549 and 293T) were
295 developed in-house. Expression and surface localization of the ACE2 protein were confirmed
296 by Western blotting (**Figure 1A**) and flow cytometry (**Figure 1B**), respectively.

297

298 *ACE2 acts as a receptor for HCoV-NL63 and is sufficient to enable infectious entry*

299 Human cell lines expressing the ACE2 protein were used to determine whether surface
300 expression of ACE2 is sufficient for HCoV-NL63 entry. Both ACE2⁺ and WT A549
301 and 293T cells were infected with HCoV-NL63 and cultured for 6 days at 32°C. Infection of
302 A549_ACE2⁺ cells resulted in clear CPE at 3 days p.i.; no CPE was observed in
303 HCoV-NL63-infected A549_WT cells and 293T_WT/ACE2⁺ cells (**Figures 2A** and **2B**,
304 respectively).

305 Despite the apparent lack of CPE in HCoV-NL63-infected 293T_ACE2⁺ cells up to
306 7 days p. i., the virus replication was examined by Western blotting with antibodies specific
307 for the NL63-N protein. The results showed that viral protein was detectable in 293T_ACE2⁺
308 and A549_ACE2⁺ cells, suggesting that expression of the ACE2 protein rendered these cell
309 lines permissive to infection by HCoV-NL63. No NL63-N protein was detected in WT cell
310 lines (**Figure 3**).

311 Coronaviruses employ discontinuous replication strategy to generate sg mRNAs during
312 minus strand synthesis; these mRNAs are then copied into plus strand mRNAs. Plus stranded
313 sg mRNA molecules are formed exclusively during virus replication and may therefore serve
314 as markers for an active infection. Thus, we next examined WT and ACE2⁺ cells for the
315 presence of each HCoV-NL63 sg mRNAs after virus inoculation. As shown in **Figure 4A**,
316 HCoV-NL63 sg mRNAs were formed in A549 and 293T cell lines expressing the ACE2
317 protein. Five mRNAs encoding viral structural and accessory proteins (spike (S), ORF3
318 protein (ORF3), envelope (E), membrane (M) and nucleocapsid (N)) and genomic RNA were
319 present, indicating active virus replication. No replication was noted in WT cells. These
320 results confirm that ACE2 may act as a functional receptor for HCoV-NL63 virus.

321 Last but not least, viral replication kinetics was assessed by real-time PCR in cell lines
322 supporting HCoV-NL63 replication (**Figure 4B**). The results confirmed virus replication and
323 progeny production in A549_ACE2⁺ cells; a steep rise in the number of viral copies in the
324 culture medium was observed already on day 3 p.i., corresponding in time with the first signs
325 of CPE. No CPE or significant increase in viral yield was observed in 293T_WT/ACE2⁺.

326

327 *Adhesion of HCoV-NL63 to mammalian cells*

328 Next, a set of experiments to determine whether ACE2 serves as an attachment factor
329 for HCoV-NL63 was performed. To address this, A549_WT and A549_ACE⁺ cells were
330 incubated at 4°C with gradient-purified HCoV-NL63 and virus adhesion to the cell surface
331 was examined using flow cytometry. The virus bound to both cell lines, suggesting that a cell
332 surface molecule other than ACE2 must be responsible for adhesion (**Figure 5**).

333 Similarly, naturally permissive, normal and PMA-treated (31) LLC-Mk2 cells were
334 incubated at 4°C with gradient-purified HCoV-NL63 and virus adhesion to cell surface was
335 examined by flow cytometry. Even though PMA-mediated ACE2 scission inhibited

336 replication of HCoV-NL63 (**Figure 6A**), we observed no difference in virus attachment to
337 normal and PMA-treated cells (**Figure 6B**). Likewise, decrease in cell surface ACE2 protein
338 levels on LLC-Mk2 cells after PMA treatment was confirmed by flow cytometry
339 (**Figure 6C**).

340 To confirm the flow cytometry results, we used confocal microscopy to examine
341 HCoV-NL63 adhesion to PMA-stimulated and normal LLC-Mk2 cells. A representative
342 image is presented in **Figure 6D**, which confirms that ACE2 shedding does not affect
343 HCoV-NL63 binding to the cell surface.

344

345 *Sialic acid or sugars moieties do not function as attachment receptor for HCoV-NL63*

346 The results outlined above suggest that another molecule on the cell surface is
347 responsible for virion attachment. Therefore, the role of sialic acid in virus adhesion was
348 examined. To this end, HCoV-NL63 replication was analyzed in cells pre-incubated with
349 *C. perfringens* type V neuraminidase, which shows a broad specificity for sialic
350 acid-containing substrates (32). Flow cytometric analysis of HCoV-NL63 adhesion to
351 LLC-Mk2 cells pre-incubated with neuraminidase showed no difference between control cells
352 and cells lacking sialic acids and ACE2 (**Figure 7A-C**). To ensure that sialic acid was
353 enzymatically removed, influenza virus was used as a positive control. As expected, a
354 significant inhibition of virus replication on A549 cells was observed after neuraminidase
355 treatment, as this common carbohydrate moiety represents a functional receptor for influenza
356 viruses (data not shown).

357 Comparable experiments were undertaken to analyze whether lectins are responsible for
358 HCoV-NL63 attachment to target cells. For this, several sugar monomers, such as D-(+)-
359 galactose, D-(+)-mannose, D-(+)-N-acetylglucosamine, L-(-)-fucose (33-35) were used in
360 virus adhesion experiments on LLC-Mk2 cells. Additionally, D-(+)-glucose, a carbohydrate

361 monomer, which does not constitute a ligand for known mammalian lectins, was included as a
362 negative control. HCoV-NL63 adhesion to LLC-Mk2 in the presence of selected sugar
363 moieties was analyzed using flow cytometry. No modulation of virus adhesion to cell surface
364 was observed (**Figure 7D-H**).

365

366 *Heparan sulfate inhibits virus attachment and entry*

367 As HS proteoglycans are important for entry of several pathogens (36-50), a soluble HS
368 was used to assess whether attachment of HCoV-NL63 is mediated by these molecules. Flow
369 cytometric analysis demonstrated that in the presence of HS virus adhesion to LLC-Mk2 cells
370 was fully inhibited, showing the role of this molecule in adhesion to susceptible cells and
371 possibly also in cell entry (**Figure 8A**).

372 In order to analyze whether ACE2 protein participates in virus attachment process,
373 additional experiments were performed. For this, virus adhesion was analyzed in the presence
374 of HS (to avoid the masking effect) on LLC-Mk2 cells with surface expression of ACE2
375 (DMSO-treated) and ACE2-deprived (PMA-treated). Inhibition of virus-HS proteoglycans
376 interaction resulted in lack of virus binding also on ACE2⁺ cells; no difference between
377 ACE2⁺ and ACE2⁻ was noted (**Figure 8A**). Flow cytometry results were further confirmed by
378 confocal microscopy (**Figure 8B**).

379 Subsequent analysis showed that pre-incubation of the virus with HS results in a dose-
380 dependent decline virus replication (**Figure 9**). Taken together, obtained results show that
381 HS proteoglycans act as HCoV-NL63 adhesion receptors and their presence is important for
382 virus entry and replication.

383

384 **DISCUSSION**

385 Human coronavirus NL63 was first identified ~10 years ago. Since then, a number of
386 research groups have studied this pathogen, resulting in the publication of a considerable
387 number of papers about the virus' epidemiology and biology. Although at first glance
388 HCoV-NL63 may simply be considered a close relative of HCoV-229E, the virus possesses
389 several unique characteristics. The most striking is that it is the only α -coronavirus to use the
390 ACE2 protein for cellular entry (similarly to SARS-CoV). Because these two pathogens use
391 the same receptor, some wonder why SARS-CoV infection manifests as life-threatening acute
392 respiratory syndrome, while HCoV-NL63 infection results in a common cold. One hypothesis
393 presented by Glowacka *et al.* assumes that HCoV-NL63-S shows only low affinity for the
394 ACE2 protein; therefore, its infection efficiency is sub-optimal (20). However, Wu *et al.*
395 showed that the affinity of NL63-S for ACE2 is comparable with that of SARS-S (51). This
396 discrepancy may result from the fact that Glowacka *et al.* used the complete S1 domain of
397 HCoV-NL63-S, while Wu *et al.* used only the receptor-binding domain (RBD). Furthermore,
398 in contrast to HCoV-NL63 infection, SARS-CoV infection results in a marked
399 down-regulation of ACE2 expression on the cell surface, thereby disrupting RAS
400 homeostasis; this in itself may cause severe lung injury (20). Dijkman *et al.* showed that
401 ACE2 expression was down-regulated upon HCoV-NL63 infection, although the result was
402 heavily dependent upon the infection efficiency (52). Based on these reports, one wonders
403 whether ACE2 is actually the cellular receptor for HCoV-NL63. The surface plasmon studies
404 previously published by Glowacka *et al.* and Wu *et al.* may suggest that NL63-S-RBD may
405 interact with ACE2; however, another stimulus may be required to expose the RBD and
406 enable its interaction with the ACE2. That would suggest similar strategy as one employed by
407 HIV-1, where CD₄ binding by gp120 results in structural alteration of the viral protein, which
408 enables gp120 binding to co-receptors and subsequent entry (53).

409 Here, we showed that directed expression of ACE2 on cells previously resistant to
410 HCoV-NL63 infection renders them susceptible. Next, we examined whether viral adherence
411 was dependent upon the level of ACE2 expression. Comparative analyses using
412 gradient-purified virus, WT cells, and cells overexpressing ACE2 showed that although
413 ACE2 protein is a pre-requisite for virus infection, it does not affect binding of virions to the
414 cell surface. Also selective scission of the ACE2 protein from the cell surface does not affect
415 the virus-cell interaction.

416 These observations are consistent with those reports showing that NL63-S protein has
417 low affinity for ACE2, and suggest that another molecule/set of molecules may serve as
418 attachment factors. In some β -coronaviruses, sialic acid may function as such a factor;
419 however, we found that removing these surface molecules with neuraminidase had no effect
420 on HCoV-NL63 replication or attachment. Similarly, soluble sugars that should hinder the
421 interaction between the potential lectin-like domain and cellular glycoproteins did not affect
422 virus binding (33-35).

423 It has been reported that some β and γ coronaviruses (SARS-CoV, culture adapted
424 MHV, IBV) employ HS proteoglycans for adhesion or entry to susceptible cells (48-50).
425 Therefore the adhesion of the virus was evaluated in the presence of HS – a soluble receptor
426 analog. Apparently, this compound blocked the ability of HCoV-NL63 to bind to the cell
427 surface of susceptible cell showing that HS proteoglycans are responsible for virus binding on
428 cells. What is more, the presence of HS proteoglycans strongly enhances virus infection,
429 showing the relevance of the observed phenomena.

430 One may, however, question whether ability of HS binding was not acquired due to cell
431 culture adaptation, as described for other coronaviral species (49, 54, 55). Analysis of the
432 S gene shows that despite *in vitro* propagation of the Amsterdam I strain, no new potential HS
433 binding sites can be identified compared to clinical isolates (data not shown). It is possible,

434 however, that different HCoV-NL63 strains bind the HS with different affinity, what would
435 explain the difficulty in acquiring new clinical isolates and late identification of the pathogen
436 (56, 57).

437 In summary, we examined whether human ACE2 (the receptor for HCoV-NL63) also
438 serves as an attachment factor. HCoV-NL63 adhered equally well to ACE2-expressing and
439 non-expressing cells. These observations indicated the existence of an additional molecule
440 involved in HCoV-NL63 attachment to target cells. Competition experiments using a range of
441 soluble elements of cellular membrane-associated components revealed that
442 HS proteoglycans constitute HCoV-NL63 adhesion receptors. Importantly, the interaction of
443 the virus with HS proteoglycans is important not only for virus binding, but also for its
444 replication.

445

446 **ACKNOWLEDGEMENTS**

447 This work was supported by a LIDER grant from the National Centre for Research and
448 Development (Lider/27/55/L-2/10/2011), a grant from the Ministry of Science and Higher
449 Education, Poland (Iuventus Plus grant IP2011 044371), and grants from the National Science
450 Center (UMO-2012/07/E/NZ6/01712; UMO-2012/07/N/NZ6/02955). The Faculty of
451 Biochemistry, Biophysics and Biotechnology at Jagiellonian University is a beneficiary of
452 structural funds from the European Union (grant no: POIG.02.01.00-12-064/08 – “Molecular
453 Biotechnology for Health”).

454
455
456
457
458
459
460
461
462
463
464
465
466
467
468
469
470
471
472
473
474
475
476
477
478
479
480
481
482
483
484
485
486
487
488
489
490
491
492
493
494
495
496
497
498
499
500
501
502
503

Reference List

1. Fields BN, Knipe DM, Howley PM. 2013. *Fields virology*, 6th ed. Wolters Kluwer/Lippincott Williams & Wilkins Health, Philadelphia.
2. Peiris JS, Yuen KY, Osterhaus AD, Stohr K. 2003. The severe acute respiratory syndrome. *The New England journal of medicine* 349:2431-2441.
3. Stadler K, Massignani V, Eickmann M, Becker S, Abrignani S, Klenk HD, Rappuoli R. 2003. SARS--beginning to understand a new virus. *Nature reviews. Microbiology* 1:209-218.
4. de Groot RJ, Baker SC, Baric RS, Brown CS, Drosten C, Enjuanes L, Fouchier RA, Galiano M, Gorbalenya AE, Memish ZA, Perlman S, Poon LL, Snijder EJ, Stephens GM, Woo PC, Zaki AM, Zambon M, Ziebuhr J. 2013. Middle East respiratory syndrome coronavirus (MERS-CoV): announcement of the Coronavirus Study Group. *Journal of virology* 87:7790-7792.
5. Fouchier RA, Hartwig NG, Bestebroer TM, Niemeyer B, de Jong JC, Simon JH, Osterhaus AD. 2004. A previously undescribed coronavirus associated with respiratory disease in humans. *Proceedings of the National Academy of Sciences of the United States of America* 101:6212-6216.
6. van der Hoek L, Pyrc K, Jebbink MF, Vermeulen-Oost W, Berkhout RJ, Wolthers KC, Wertheim-van Dillen PM, Kaandorp J, Spaargaren J, Berkhout B. 2004. Identification of a new human coronavirus. *Nature medicine* 10:368-373.
7. Pyrc K, Berkhout B, van der Hoek L. 2007. The novel human coronaviruses NL63 and HKU1. *Journal of virology* 81:3051-3057.
8. van der Hoek L, Sure K, Ihorst G, Stang A, Pyrc K, Jebbink MF, Petersen G, Forster J, Berkhout B, Uberla K. 2006. Human coronavirus NL63 infection is associated with croup. *Advances in experimental medicine and biology* 581:485-491.
9. van der Hoek L, Sure K, Ihorst G, Stang A, Pyrc K, Jebbink MF, Petersen G, Forster J, Berkhout B, Uberla K. 2005. Croup is associated with the novel coronavirus NL63. *PLoS medicine* 2:e240.
10. Pyrc K, Jebbink MF, Berkhout B, van der Hoek L. 2004. Genome structure and transcriptional regulation of human coronavirus NL63. *Virology journal* 1:7.
11. Pyrc K, Dijkman R, Deng L, Jebbink MF, Ross HA, Berkhout B, van der Hoek L. 2006. Mosaic structure of human coronavirus NL63, one thousand years of evolution. *Journal of molecular biology* 364:964-973.
12. Gallagher TM, Buchmeier MJ. 2001. Coronavirus spike proteins in viral entry and pathogenesis. *Virology* 279:371-374.
13. Zheng Q, Deng Y, Liu J, van der Hoek L, Berkhout B, Lu M. 2006. Core structure of S2 from the human coronavirus NL63 spike glycoprotein. *Biochemistry* 45:15205-15215.
14. Hofmann H, Pyrc K, van der Hoek L, Geier M, Berkhout B, Pohlmann S. 2005. Human coronavirus NL63 employs the severe acute respiratory syndrome coronavirus receptor for cellular entry. *Proceedings of the National Academy of Sciences of the United States of America* 102:7988-7993.
15. Hofmann H, Marzi A, Gramberg T, Geier M, Pyrc K, van der Hoek L, Berkhout B, Pohlmann S. 2006. Attachment factor and receptor engagement of SARS coronavirus and human coronavirus NL63. *Advances in experimental medicine and biology* 581:219-227.
16. Pohlmann S, Gramberg T, Wegele A, Pyrc K, van der Hoek L, Berkhout B, Hofmann H. 2006. Interaction between the spike protein of human coronavirus NL63 and its cellular receptor ACE2. *Advances in experimental medicine and biology* 581:281-284.
17. Donoghue M, Hsieh F, Baronas E, Godbout K, Gosselin M, Stagliano N, Donovan M, Woolf B, Robison K, Jeyaseelan R, Breitbart RE, Acton S. 2000. A novel angiotensin-converting enzyme-related carboxypeptidase (ACE2) converts angiotensin I to angiotensin 1-9. *Circulation research* 87:E1-9.

- 504 18. Rice GI, Thomas DA, Grant PJ, Turner AJ, Hooper NM. 2004. Evaluation of angiotensin-
505 converting enzyme (ACE), its homologue ACE2 and neprilysin in angiotensin peptide
506 metabolism. *The Biochemical journal* 383:45-51.
- 507 19. Tipnis SR, Hooper NM, Hyde R, Karran E, Christie G, Turner AJ. 2000. A human homolog of
508 angiotensin-converting enzyme. Cloning and functional expression as a captopril-
509 insensitive carboxypeptidase. *The Journal of biological chemistry* 275:33238-33243.
- 510 20. Glowacka I, Bertram S, Herzog P, Pfefferle S, Steffen I, Muench MO, Simmons G, Hofmann
511 H, Kuri T, Weber F, Eichler J, Drosten C, Pohlmann S. 2010. Differential downregulation of
512 ACE2 by the spike proteins of severe acute respiratory syndrome coronavirus and human
513 coronavirus NL63. *Journal of virology* 84:1198-1205.
- 514 21. Kuba K, Imai Y, Rao S, Gao H, Guo F, Guan B, Huan Y, Yang P, Zhang Y, Deng W, Bao L,
515 Zhang B, Liu G, Wang Z, Chappell M, Liu Y, Zheng D, Leibbrandt A, Wada T, Slutsky AS, Liu
516 D, Qin C, Jiang C, Penninger JM. 2005. A crucial role of angiotensin converting enzyme 2
517 (ACE2) in SARS coronavirus-induced lung injury. *Nature medicine* 11:875-879.
- 518 22. Li W, Moore MJ, Vasilieva N, Sui J, Wong SK, Berne MA, Somasundaran M, Sullivan JL,
519 Luzuriaga K, Greenough TC, Choe H, Farzan M. 2003. Angiotensin-converting enzyme 2 is a
520 functional receptor for the SARS coronavirus. *Nature* 426:450-454.
- 521 23. Li W, Sui J, Huang IC, Kuhn JH, Radoshitzky SR, Marasco WA, Choe H, Farzan M. 2007. The S
522 proteins of human coronavirus NL63 and severe acute respiratory syndrome coronavirus
523 bind overlapping regions of ACE2. *Virology* 367:367-374.
- 524 24. Hattermann K, Muller MA, Nitsche A, Wendt S, Donoso Mantke O, Niedrig M. 2005.
525 Susceptibility of different eukaryotic cell lines to SARS-coronavirus. *Archives of virology*
526 150:1023-1031.
- 527 25. Hofmann H, Hattermann K, Marzi A, Gramberg T, Geier M, Krumbiegel M, Kuate S, Uberla
528 K, Niedrig M, Pohlmann S. 2004. S protein of severe acute respiratory syndrome-associated
529 coronavirus mediates entry into hepatoma cell lines and is targeted by neutralizing
530 antibodies in infected patients. *Journal of virology* 78:6134-6142.
- 531 26. Schildgen O, Jebbink MF, de Vries M, Pyrc K, Dijkman R, Simon A, Muller A, Kupfer B, van
532 der Hoek L. 2006. Identification of cell lines permissive for human coronavirus NL63.
533 *Journal of virological methods* 138:207-210.
- 534 27. Mathewson AC, Bishop A, Yao Y, Kemp F, Ren J, Chen H, Xu X, Berkhout B, van der Hoek L,
535 Jones IM. 2008. Interaction of severe acute respiratory syndrome-coronavirus and NL63
536 coronavirus spike proteins with angiotensin converting enzyme-2. *The Journal of general*
537 *virology* 89:2741-2745.
- 538 28. Moffat J, Grueneberg DA, Yang X, Kim SY, Kloepper AM, Hinkle G, Piqani B, Eisenhaure TM,
539 Luo B, Grenier JK, Carpenter AE, Foo SY, Stewart SA, Stockwell BR, Hacohen N, Hahn WC,
540 Lander ES, Sabatini DM, Root DE. 2006. A lentiviral RNAi library for human and mouse
541 genes applied to an arrayed viral high-content screen. *Cell* 124:1283-1298.
- 542 29. Reed LJ, Muench H. 1938. A simple method of estimating fifty per cent endpoints. *Am. J.*
543 *Epidemiol.* 27:493-497.
- 544 30. Bolte S, Cordelieres FP. 2006. A guided tour into subcellular colocalization analysis in light
545 microscopy. *Journal of microscopy* 224:213-232.
- 546 31. Lai ZW, Hanchapola I, Steer DL, Smith AI. 2011. Angiotensin-converting enzyme 2
547 ectodomain shedding cleavage-site identification: determinants and constraints.
548 *Biochemistry* 50:5182-5194.
- 549 32. Rauvala H. 1979. Monomer-micelle transition of the ganglioside GM1 and the hydrolysis by
550 *Clostridium perfringens* neuraminidase. *European journal of biochemistry / FEBS* 97:555-
551 564.
- 552 33. Klimstra WB, Nangle EM, Smith MS, Yurochko AD, Ryman KD. 2003. DC-SIGN and L-SIGN
553 can act as attachment receptors for alphaviruses and distinguish between mosquito cell-
554 and mammalian cell-derived viruses. *Journal of virology* 77:12022-12032.

- 555 34. Alvarez CP, Lasala F, Carrillo J, Muniz O, Corbi AL, Delgado R. 2002. C-type lectins DC-SIGN
556 and L-SIGN mediate cellular entry by Ebola virus in cis and in trans. *Journal of virology*
557 76:6841-6844.
- 558 35. Zhang Y, Buckles E, Whittaker GR. 2012. Expression of the C-type lectins DC-SIGN or L-SIGN
559 alters host cell susceptibility for the avian coronavirus, infectious bronchitis virus.
560 *Veterinary microbiology* 157:285-293.
- 561 36. Sureau C, Salisse J. 2013. A conformational heparan sulfate binding site essential to
562 infectivity overlaps with the conserved hepatitis B virus a-determinant. *Hepatology* 57:985-
563 994.
- 564 37. Lamas Longarela O, Schmidt TT, Schoneweis K, Romeo R, Wedemeyer H, Urban S, Schulze
565 A. 2013. Proteoglycans act as cellular hepatitis delta virus attachment receptors. *PloS one*
566 8:e58340.
- 567 38. Kobayashi K, Kato K, Sugi T, Takemae H, Pandey K, Gong H, Tohya Y, Akashi H. 2010.
568 *Plasmodium falciparum* BAEBL binds to heparan sulfate proteoglycans on the human
569 erythrocyte surface. *The Journal of biological chemistry* 285:1716-1725.
- 570 39. Bucior I, Pielage JF, Engel JN. 2012. *Pseudomonas aeruginosa* pili and flagella mediate
571 distinct binding and signaling events at the apical and basolateral surface of airway
572 epithelium. *PLoS pathogens* 8:e1002616.
- 573 40. Norman MU, Moriarty TJ, Dresser AR, Millen B, Kubes P, Chaconas G. 2008. Molecular
574 mechanisms involved in vascular interactions of the Lyme disease pathogen in a living host.
575 *PLoS pathogens* 4:e1000169.
- 576 41. Lebrun P, Raze D, Fritzinger B, Wieruszkeski JM, Biet F, Dose A, Carpentier M, Schwarzer D,
577 Allain F, Lippens G, Loch C. 2012. Differential contribution of the repeats to heparin
578 binding of HBHA, a major adhesin of *Mycobacterium tuberculosis*. *PloS one* 7:e32421.
- 579 42. Germe R, Crance JM, Garin D, Guimet J, Lortat-Jacob H, Ruigrok RW, Zarski JP, Drouet E.
580 2002. Cellular glycosaminoglycans and low density lipoprotein receptor are involved in
581 hepatitis C virus adsorption. *Journal of medical virology* 68:206-215.
- 582 43. Kalia M, Chandra V, Rahman SA, Sehgal D, Jameel S. 2009. Heparan sulfate proteoglycans
583 are required for cellular binding of the hepatitis E virus ORF2 capsid protein and for viral
584 infection. *Journal of virology* 83:12714-12724.
- 585 44. Cruz L, Meyers C. 2013. Differential dependence on host cell glycosaminoglycans for
586 infection of epithelial cells by high-risk HPV types. *PloS one* 8:e68379.
- 587 45. Shukla D, Liu J, Blaiklock P, Shworak NW, Bai X, Esko JD, Cohen GH, Eisenberg RJ,
588 Rosenberg RD, Spear PG. 1999. A novel role for 3-O-sulfated heparan sulfate in herpes
589 simplex virus 1 entry. *Cell* 99:13-22.
- 590 46. Lambert S, Bouttier M, Vassy R, Seigneuret M, Petrow-Sadowski C, Janvier S, Heveker N,
591 Ruscetti FW, Perret G, Jones KS, Pique C. 2009. HTLV-1 uses HSPG and neuropilin-1 for
592 entry by molecular mimicry of VEGF165. *Blood* 113:5176-5185.
- 593 47. Patel M, Yanagishita M, Roderiquez G, Bou-Habib DC, Oravec T, Hascall VC, Norcross MA.
594 1993. Cell-surface heparan sulfate proteoglycan mediates HIV-1 infection of T-cell lines.
595 *AIDS research and human retroviruses* 9:167-174.
- 596 48. Watanabe R, Sawicki SG, Taguchi F. 2007. Heparan sulfate is a binding molecule but not a
597 receptor for CEACAM1-independent infection of murine coronavirus. *Virology* 366:16-22.
- 598 49. Madu IG, Chu VC, Lee H, Regan AD, Bauman BE, Whittaker GR. 2007. Heparan sulfate is a
599 selective attachment factor for the avian coronavirus infectious bronchitis virus Beaudette.
600 *Avian diseases* 51:45-51.
- 601 50. Lang J, Yang N, Deng J, Liu K, Yang P, Zhang G, Jiang C. 2011. Inhibition of SARS pseudovirus
602 cell entry by lactoferrin binding to heparan sulfate proteoglycans. *PloS one* 6:e23710.
- 603 51. Wu K, Chen L, Peng G, Zhou W, Pennell CA, Mansky LM, Geraghty RJ, Li F. 2011. A virus-
604 binding hot spot on human angiotensin-converting enzyme 2 is critical for binding of two
605 different coronaviruses. *Journal of virology* 85:5331-5337.

- 606 52. Dijkman R, Jebbink MF, Deijs M, Milewska A, Pyrc K, Buelow E, van der Bijl A, van der Hoek
607 L. 2012. Replication-dependent downregulation of cellular angiotensin-converting enzyme
608 2 protein expression by human coronavirus NL63. *The Journal of general virology* 93:1924-
609 1929.
- 610 53. Wilen CB, Tilton JC, Doms RW. 2012. HIV: cell binding and entry. *Cold Spring Harbor*
611 *perspectives in medicine* 2.
- 612 54. de Haan CA, Haijema BJ, Schellen P, Wichgers Schreur P, te Lintelo E, Vennema H, Rottier
613 PJ. 2008. Cleavage of group 1 coronavirus spike proteins: how furin cleavage is traded off
614 against heparan sulfate binding upon cell culture adaptation. *Journal of virology* 82:6078-
615 6083.
- 616 55. de Haan CA, Li Z, te Lintelo E, Bosch BJ, Haijema BJ, Rottier PJ. 2005. Murine coronavirus
617 with an extended host range uses heparan sulfate as an entry receptor. *Journal of virology*
618 79:14451-14456.
- 619 56. Dijkman R, Jebbink MF, Koekkoek SM, Deijs M, Jonsdottir HR, Molenkamp R, Ieven M,
620 Goossens H, Thiel V, van der Hoek L. 2013. Isolation and characterization of current human
621 coronavirus strains in primary human epithelial cell cultures reveal differences in target cell
622 tropism. *Journal of virology* 87:6081-6090.
- 623 57. van der Hoek L, Pyrc K, Berkhout B. 2006. Human coronavirus NL63, a new respiratory
624 virus. *FEMS microbiology reviews* 30:760-773.
- 625
626
627

628 **FIGURE LEGENDS**

629 **Figure 1. Human cell lines overexpressing ACE2 protein.** (A) Lysates of A549 +/-
 630 (A549_ACE2⁺ and A549_WT) and 293T +/- (293T_ACE2⁺ and 293T_WT) cells were tested
 631 for the presence of the ACE2 protein with Western blotting using antibodies specific to the
 632 ectodomain of the human ACE2 protein. „-” and „+” signs denote wild-type and ACE2
 633 overexpressing cell lines, respectively. Concomitantly, the β -actin protein levels were
 634 assessed in each sample. Numbers on the left side represent molecular mass [kDa] assessed
 635 with a size marker. The results shown are representative of at least three independent
 636 experiments. (B) A549_ACE2⁺, A549_WT, 293T_ACE2⁺ and 293T_WT cells were tested
 637 for the surface expression of the ACE2 protein with flow cytometry using antibodies specific
 638 to the ectodomain of the human ACE2 protein. The results shown are representative of at least
 639 three independent experiments.

640

641 **Figure 2. Cytopathic effect on A549_ACE2⁺ cells during HCoV-NL63 infection.**
 642 ACE2-overexpressing (ACE2⁺) and wild type (WT) A549 and 293T cells were infected with
 643 HCoV-NL63 or inoculated with mock and cultured for 6 days. Cytopathic effect was
 644 observed only on HCoV-NL63 infected A549_ACE2⁺ cells. Magnification: 200 \times . The results
 645 shown are representative of at least three independent experiments.

646

647 **Figure 3. HCoV-NL63 nucleocapsid protein expression in ACE2⁺ cells.** ACE2⁺ and WT
 648 293T and A549 cells were infected with HCoV-NL63 (+) or mock (-). HCoV-NL63
 649 nucleocapsid protein was detected 6 days p.i. in A549_ACE2⁺ and 293T_ACE2⁺ cell lysates,
 650 suggesting viral replication. No signal from the NL63-N protein was observed in
 651 mock-infected cells. Sample containing lysate of LLC-Mk2 cells infected with HCoV-NL63
 652 was used as a positive control (PC). A position of 55 kDa a molecular mass marker is shown

653 on the left side. The results shown are representative of at least three independent
654 experiments.

655

656 **Figure 4. HCoV-NL63 replication in ACE2-overexpressing cells.** ACE2-overexpressing
657 and wild type cells were infected with HCoV-NL63 (+) or mock (-) and cultured for 6 days.

658 **(A)** Genomic RNA (1a) and a set of HCoV-NL63 sg mRNAs, including spike (S), ORF3,
659 envelope (E), membrane (M) and nucleocapsid (N), were detected in A549_ACE2⁺ and
660 293T_ACE2⁺ cells. No HCoV-NL63 sg mRNAs were detected in WT cells. LLC-Mk2 cells
661 infected with HCoV-NL63 (+) or mock (-) were used as controls. Positions of nt size markers
662 are shown on the left side of each panel. The results shown are representative of at least three
663 independent experiments. **(B)** HCoV-NL63 replication on A549 and 293T cells was evaluated
664 with real-time PCR. Marked increase in virus yield was observed on A549_ACE2⁺ and, to
665 much lesser extent, on 293T_ACE2⁺ cells. No increase in virus yield was observed on
666 HCoV-NL63-infected A549 and 293T WT cells. Data on virus replication are presented as
667 HCoV-NL63 RNA copies/ml. All assays were performed in triplicate and average values with
668 standard errors (error bars) are presented.

669

670 **Figure 5. Directed expression of the ACE2 protein on A549 cells does not alter HCoV-**
671 **NL63 adhesion.** Analysis of HCoV-NL63 adherence to ACE2-overexpressing (ACE2⁺) or
672 wild type (WT) A549 cells was conducted with flow cytometry. The results shown are
673 representative of at least three independent experiments.

674

675 **Figure 6. Adherence of HCoV-NL63 to LLC-Mk2 cells deprived of the ACE2 protein.**

676 LLC-Mk2 cells were deprived of surface ACE2 protein by incubation with 1 μ M PMA and
677 subsequently incubated with purified HCoV-NL63 or mock. DMSO-treated cells were used as

678 a control. **(A)** HCoV-NL63 replication on LLC-MK2 ACE2⁺ and ACE2⁻ cells was evaluated
 679 with real-time PCR. A significant decrease in viral replication was observed on LLC-MK2
 680 cells pre-treated with PMA, compared to control cells. Data on virus replication are presented
 681 as HCoV-NL63 RNA copies/ml. **(B)** Analysis of HCoV-NL63 adherence to ACE2^{+/} LLC-
 682 MK2 cells. HCoV-NL63 was labelled with specific antibodies and virus adhesion was
 683 analyzed with flow cytometry. **(C)** A decrease in surface expression of the ACE2 protein on
 684 LLC-MK2 after PMA treatment was confirmed using flow cytometry. **(D)** HCoV-NL63
 685 adhesion to ACE2^{+/} LLC-Mk2 cells was confirmed by confocal microscopy. LLC-MK2 cells
 686 were pre-treated with PMA [**PMA**] or DMSO [**DMSO**] and incubated with purified HCoV-
 687 NL63. HCoV-NL63 virions are presented in green, while the blue color denotes DNA. Each
 688 image is a single confocal plane (xy) with two orthogonal views (xz and yz) created by
 689 maximum projection of axial planes (thickness 0.7 μm). Scale: 10 μm. The results shown are
 690 representative of at least three independent experiments.

691

692 **Figure 7. HCoV-NL63 adhesion to neuraminidase-treated cells and in the presence of**
 693 **sugar moieties.** LLC-Mk2 cells were treated with DMSO **(A)**, 1 μM PMA **(B)** or 1 μM PMA
 694 and 200 mU/ml type V neuraminidase **(C)** and further incubated with purified HCoV-NL63
 695 or mock. Virus adhesion was assessed also in the presence of 50 mM sugar monomers:
 696 galactose **(D)**, mannose **(E)**, N-acetylglucosamine **(F)**, fucose **(G)** or glucose **(H)**, as a
 697 negative control. Virus adhesion was analyzed with flow cytometry. The results shown are
 698 representative of at least three independent experiments.

699

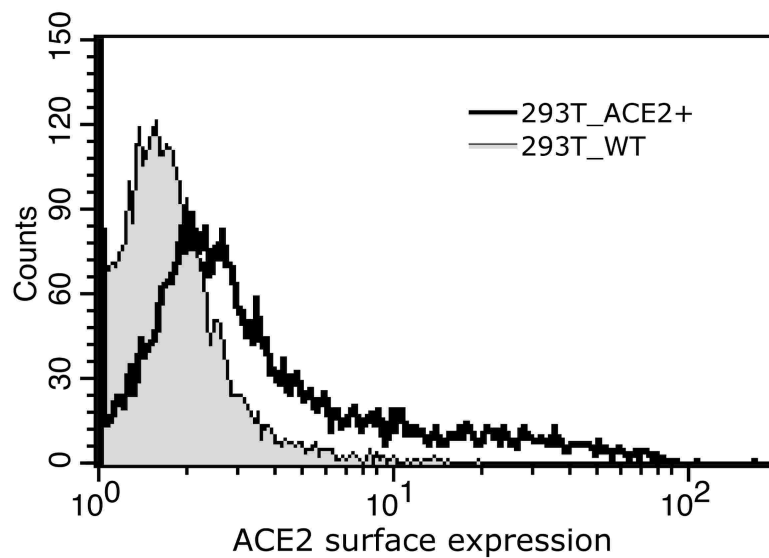
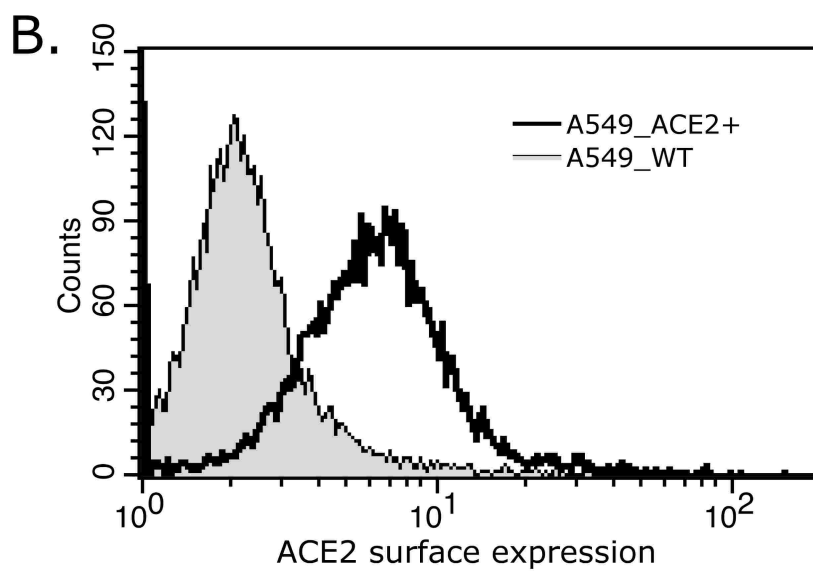
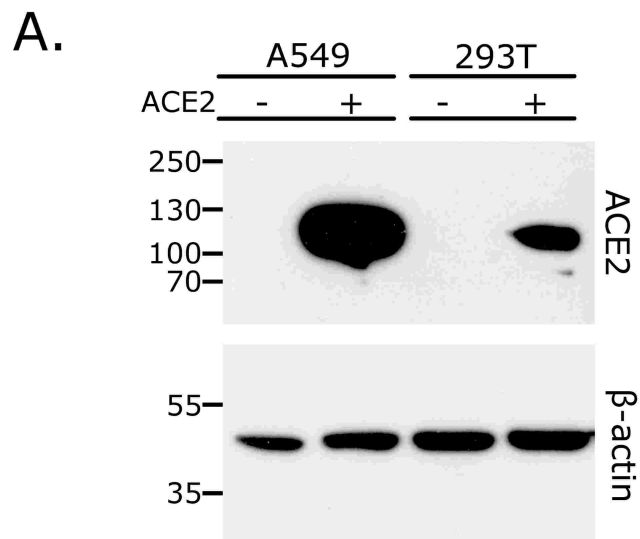
700 **Figure 8. HCoV-NL63 adhesion to ACE2⁺/ACE2⁻ cells in the presence of heparan**
 701 **sulfate.** **(A)** Flow cytometry analysis of HCoV-NL63 adhesion. The ACE2 protein was
 702 removed from the surface of LLC-Mk2 cells by incubation with 1 μM PMA (**ACE2⁻**), while

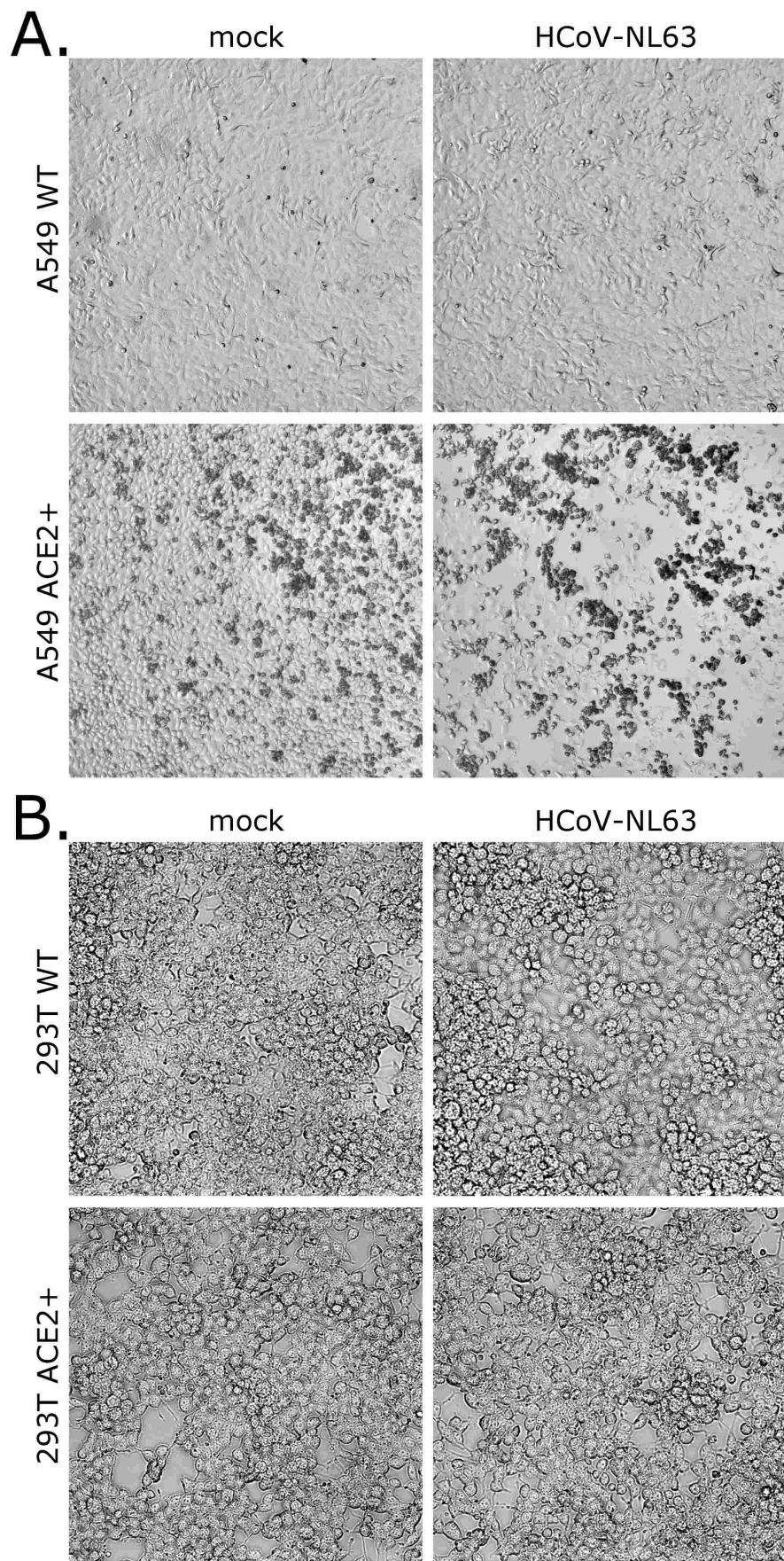
703 control cells were treated with DMSO (**ACE2**⁺). Adhesion of HCoV-NL63 was assessed on
 704 **ACE2**⁷⁺ cells in the presence of 300 µg/ml HS or control PBS. **(B)** Confocal microscopy
 705 analysis of HCoV-NL63 adhesion. LLC-MK2 cells were stimulated with 1 µM PMA [**PMA**]
 706 or DMSO and incubated with purified HCoV-NL63 [**NL63**] in the presence or absence of
 707 heparan sulfate [**HS**]. [**NC**] denotes cells incubated with mock sample. HCoV-NL63 virions
 708 are presented in green, while the blue color denotes DNA. Each image is a single confocal
 709 plane (xy) with two orthogonal views (xz and yz) created by maximum projection of axial
 710 planes (thickness 4.8 µm). Scale: 5 µm. Bars represent the mean number of virions from 10
 711 cells per sample ± standard error.

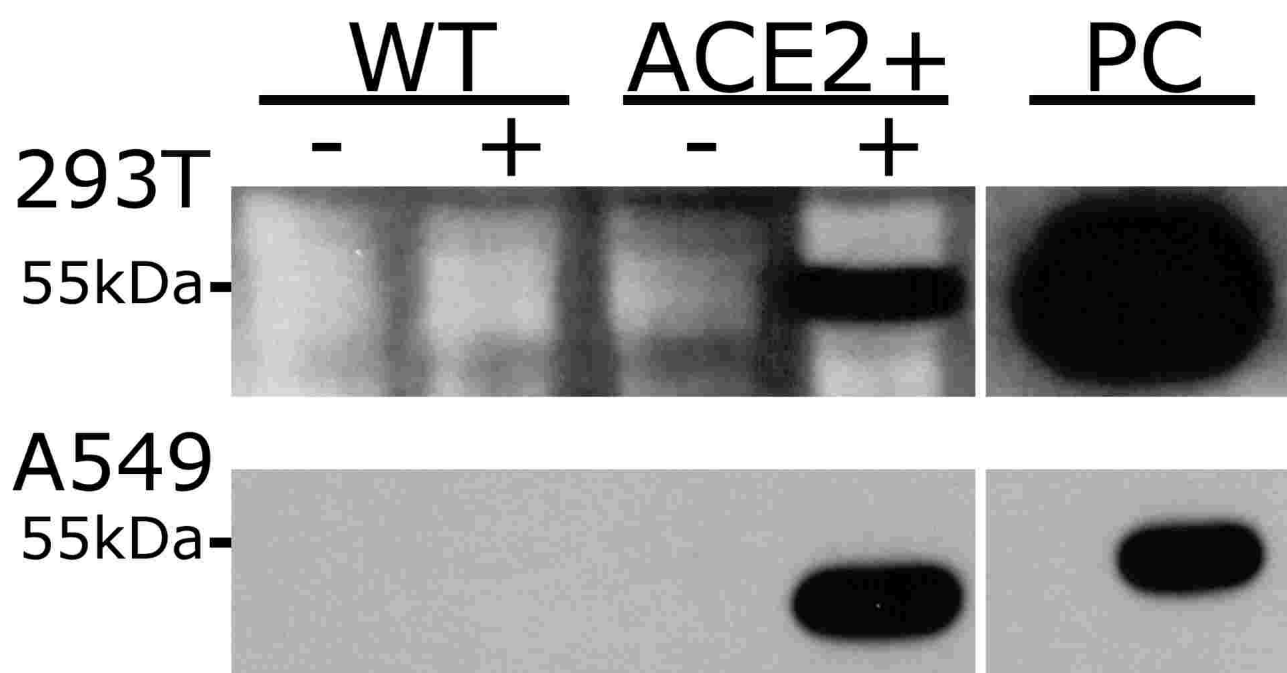
712

713 **Figure 9. HCoV-NL63 replication in the presence of heparan sulfate.** LLC-Mk2 cells
 714 were infected with HCoV-NL63 in the presence of increasing concentrations of HS or PBS.
 715 Virus replication in cell culture supernatants was evaluated using real-time PCR on day 4 p.i.
 716 Data on virus replication are presented as HCoV-NL63 RNA copies/ml. All assays were
 717 performed in triplicate and average values with standard errors (error bars) are presented. For
 718 all concentrations the decrease in virus yield is statistically significant (student's t-test;
 719 p<0.05).

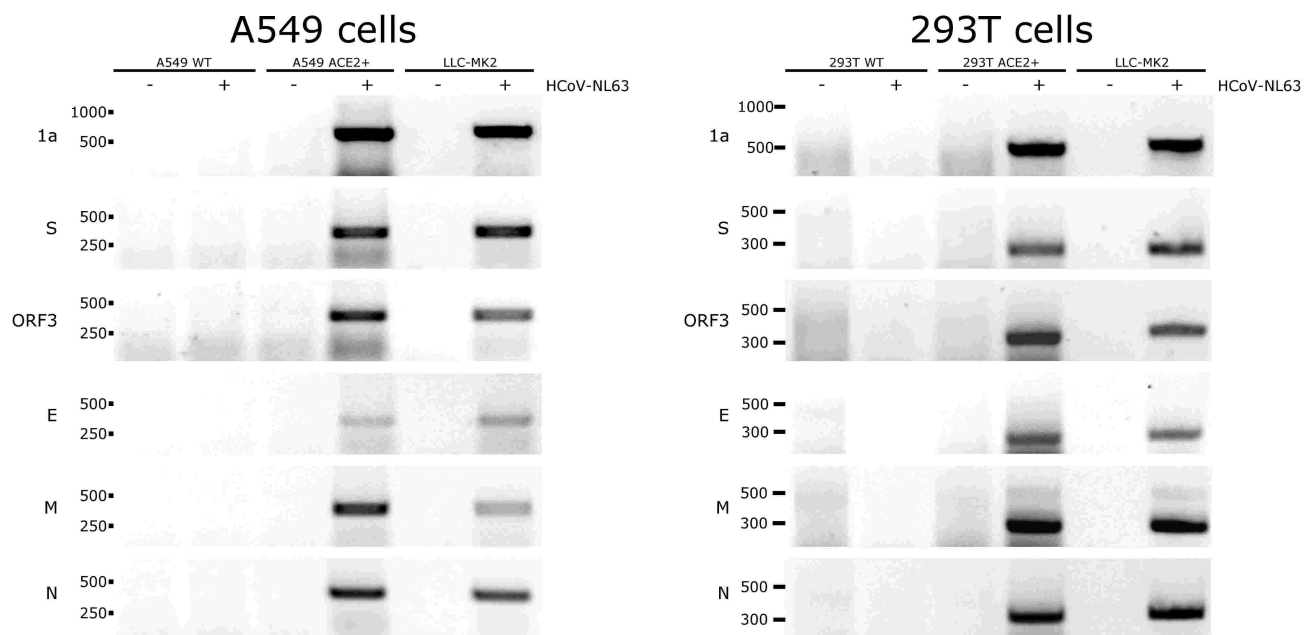
720



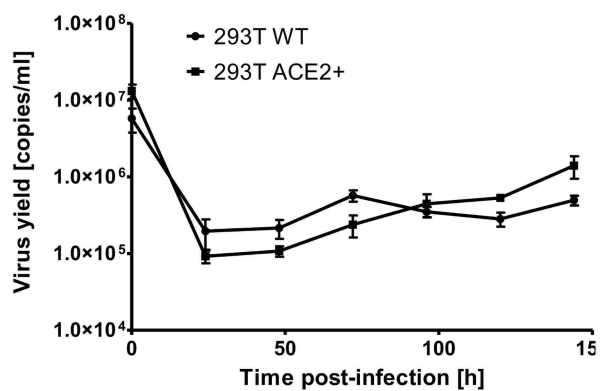
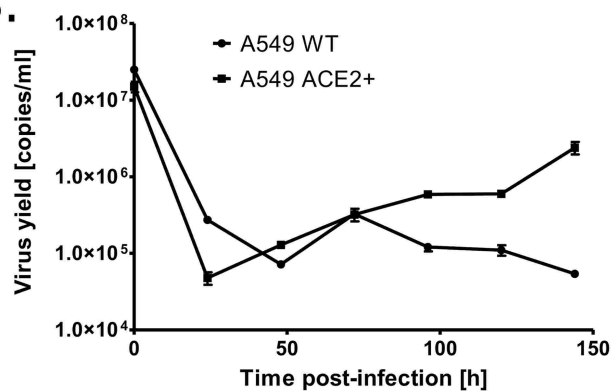


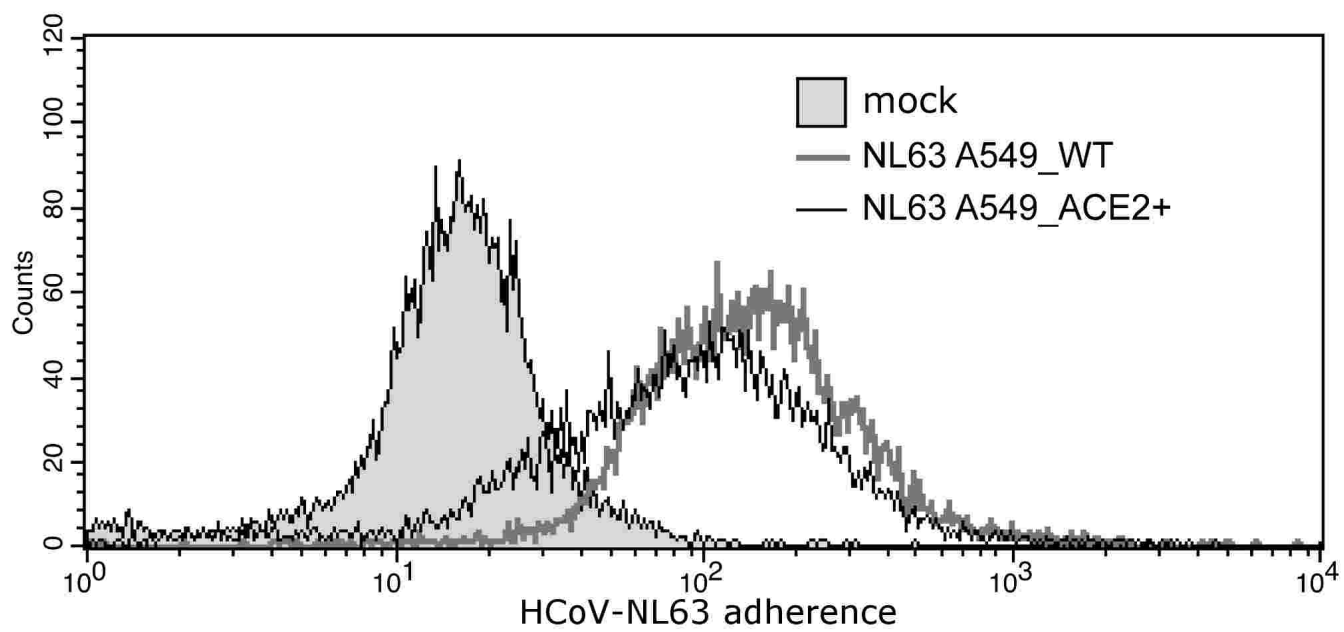


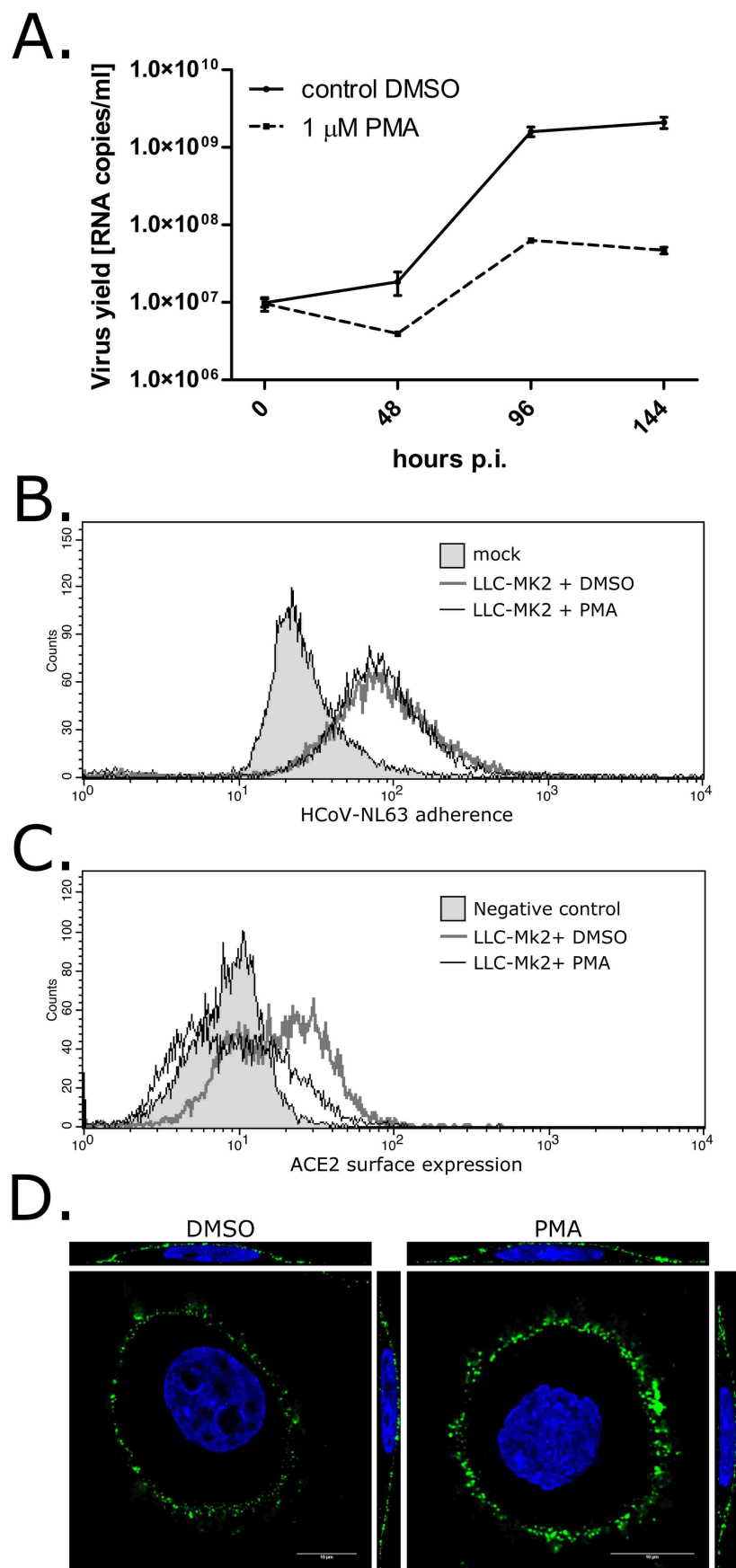
A.

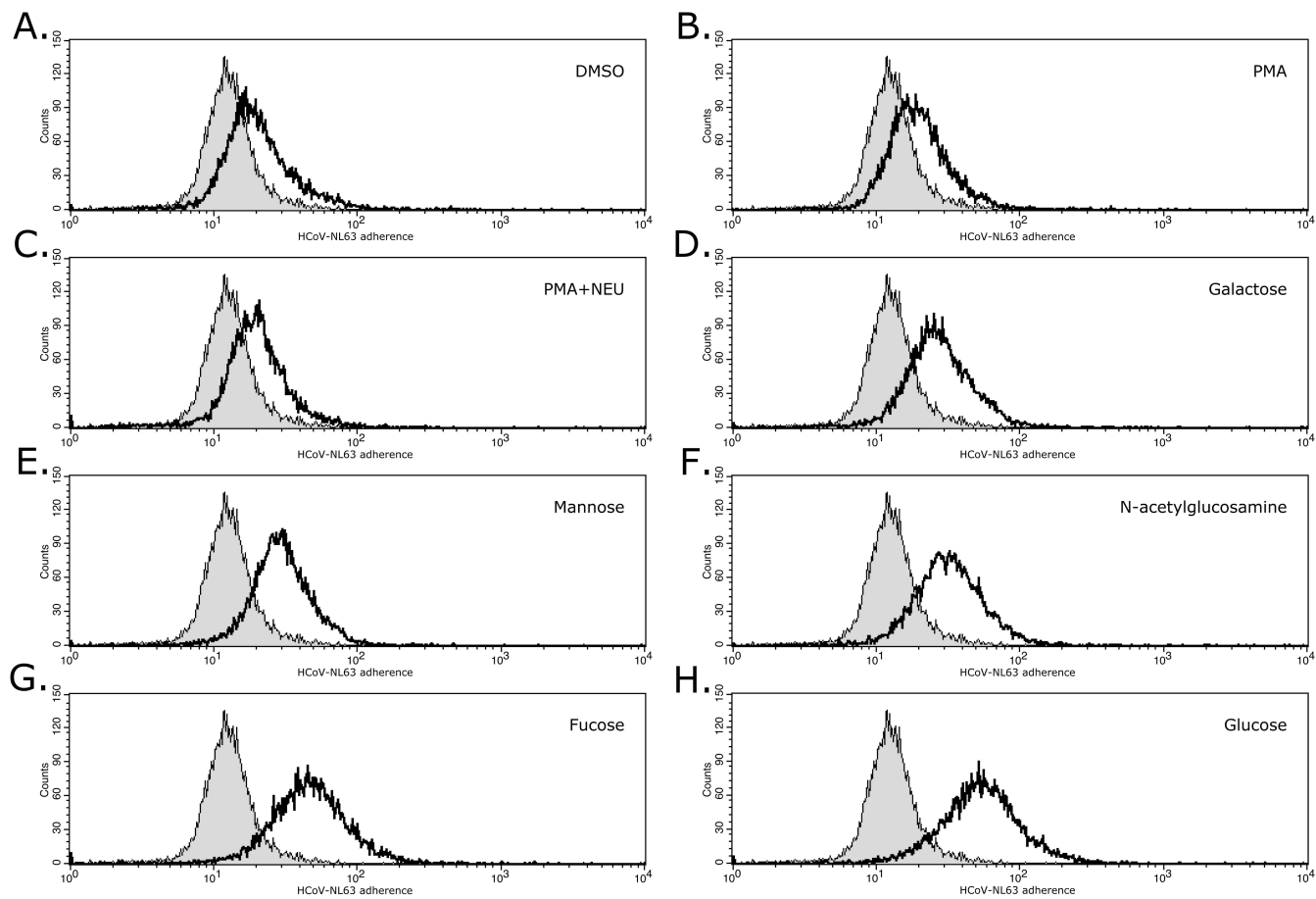


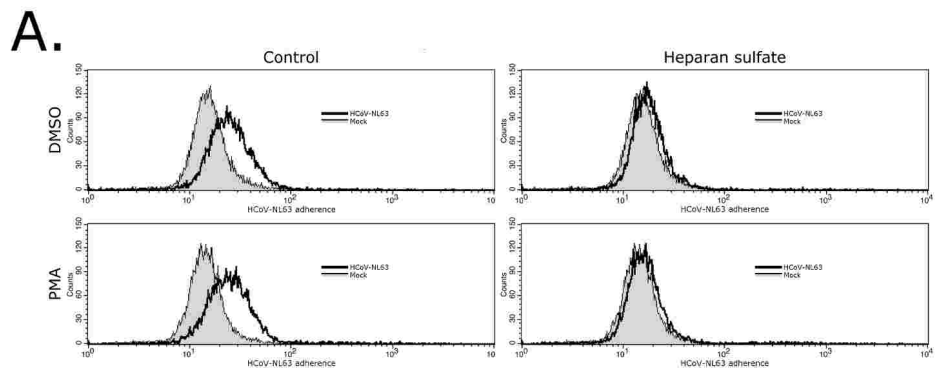
B.











B.

